Journal of Applied Mechanics and Technical Physics, Vol. 44, No. 4, pp. 461–470, 2003

INTERACTION OF A STREAMWISE VORTEX WITH AN OBLIQUE SHOCK WAVE

V. N. Zudov and E. A. Pimonov

UDC 533.69.011:533.6.011.72

Interaction of a supersonic streamwise vortex with an oblique shock wave is considered. A mathematical model of the streamwise vortex is constructed. Three interaction regimes (weak, moderate, and strong) are found. It is shown numerically that vortex breakdown is possible in the case of strong interaction. The influence of the governing parameters on the interaction type is studied. It is shown that the main effect on the interaction type is exerted by the streamwise velocity and angle of the wedge forming the shock wave. The effect of splitting of the primary vortex on the shock wave in the case of moderate and strong interaction regimes is found.

Key words: *supersonic flow, streamwise vortex, shock wave, vortex breakdown.*

Introduction. Interaction of a streamwise vortex with a shock wave is a complex three-dimensional, most often unsteady phenomenon encountered in both external flows and internal flows (inlets, nozzles, and combustors). This is the classical problem in theoretical gas dynamics and is very important for analyzing external flow around supersonic aircraft with wings of large sweep and small aspect ratio. The distinctive feature of such flows is the generation of a vortex sheet near the leading edge of the wing and its subsequent rolling into two isolated streamwise vortices that interact with shock waves formed on the aircraft surface elements. Origination of vortices is also observed in supersonic flow around a body at incidence. In this case, vortex cores are formed on the forebody; propagating downstream, the vortex cores form isolated streamwise vortices. Two isolated streamwise vortices are usually formed in the flow around a delta wing at incidence [1]. Similar streamwise vortices are formed at subsonic velocities [2]. In bodies of an aircraft configuration, such vortex structures can enter the engine inlet. Depending on the interaction mode of the streamwise vortex and the shock wave always formed ahead of a supersonic inlet, the flow-rate, drag, and other parameters of this propulsion element can be significantly changed. Such situations can lead to catastrophic consequences for a supersonic aircraft. Problems of supersonic external flow can involve a situation where the streamwise vortex interacts with the aircraft surface, which significantly alters the lifting and moment characteristics of wings and other aircraft elements. The changes in the force characteristics can result in the loss of stability and controllability of the aircraft.

The problem of interaction of a streamwise vortex with a shock wave can also arise in the study of fuel and oxidizer mixing in combustion chambers of hypersonic flying vehicles with air-breathing engines. It is assumed that such vehicles will have a supersonic flow velocity in the combustor. The problem of fuel and oxidizer mixing at supersonic velocities is extremely complicated. One method of mixing intensification is the formation of vortex cores on struts mounted at the combustor entrance and their further propagation in the combustor duct, where they interact with shock waves, which are inherent in a supersonic combustor.

It was shown in the experimental works of [3, 4] that the action of a strong external disturbance on the streamwise vortex propagating in the flow results in the so-called vortex explosion or vortex breakdown. This phenomenon was observed both in incompressible flows containing vortices and in compressible subsonic and supersonic flows. The term "vortex explosion" means the formation of a point (or a surface) of total stagnation of the flow in the region of interaction of the vortex and the strong disturbance and the formation of a reverse flow region

Institute of Theoretical and Applied Mechanics, Siberian Division, Russian Academy of Sciences, Novosibirsk 630090. Translated from Prikladnaya Mekhanika i Tekhnicheskaya Fizika, Vol. 44, No. 4, pp. 10–21, July–August, 2003. Original article submitted July 11, 2002; revision submitted October 24, 2002.

0021-8944/03/4404-0461 $25.00

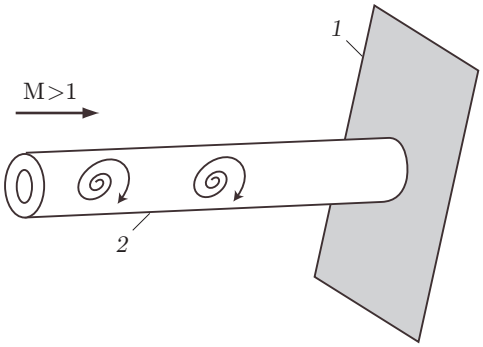

Fig. 1. Flow pattern at the time $t = 0$: 1) shock wave; 2) vortex.

(which is sometimes rather extended) near the vortex centerline. Note, even in the case of an incompressible fluid, the problem of vortex explosion has not been ultimately solved [3]. Various semi-empirical criteria for determining vortex-breakdown conditions were derived for an incompressible fluid. In the range of supersonic velocities, important results were obtained in the experiments of Zatoloka et al. [5] who put forward an assumption that the mechanisms of vortex explosion and boundary-layer separation are similar. This idea was developed by Glotov [6] who found that vortex breakdown occurs at angles of attack of the wing or a body of revolution equal to 5–10° and shock strengths close to the strength of the normal shock with a subsonic velocity behind the slip surface. Origination of unsteady oscillatory regimes in the region of interaction of the streamwise vortex and the shock wave was observed in [6, 7]. Quantitative experimental results were obtained in [4, 8]. The results of investigations confirmed the presence of recirculation zones in the interaction region. The ratio of the circular velocity to the axial velocity was used as a parameter determining the interaction mode, and data on the structure of interaction regimes were obtained. However, only one type of vortex interaction with the normal shock wave was considered. In both cases [4, 8], the circular component of velocity in an undisturbed vortex was subsonic. Leibovich [3] demonstrated the existence of two types of streamwise vortices developed in a cocurrent flow: jet-type vortices and wake-type vortices, which are characterized, respectively, by the maximum and minimum of the axial component of the velocity vector at the axis. Both types of vortices were observed in subsonic flow around various bodies in experiments [3]. In addition to the information given above, investigations [1] are known, where supersonic streamwise vortices on the leeward side of a delta wing and in the wake behind a complex-shaped body were considered. Supersonic circular components of velocity and (as in the experiments of [4, 8]) a wake-type vortex were registered experimentally.

If the streamwise vortex intersects the shock wave, interactions of two types are possible: 1) interaction of the streamwise vortex with the shock wave perpendicular to the vortex axis; 2) interaction of the streamwise vortex with the shock wave inclined to the vortex axis. The first type of interaction was experimentally studied in [4, 7, 9], and the second type was considered in [6, 9]. It was shown in these papers that, in the first case of interaction, the vortex breaks down, and a reverse flow region with flow unsteadiness appears. There are a few papers where the interaction of the streamwise vortex and the shock wave was simulated numerically. The results of these papers are contradictory. Thus, vortex–shock wave interaction regimes with vortex explosion were observed in some works [10, 11], whereas no vortex breakdown was obtained in other works [12]. Therefore, it is necessary to develop a mathematical model for a complex spatial (often unsteady) phenomenon: interaction of a streamwise vortex with a shock wave.

The objective of the present work is numerical simulation of various types of interaction of a streamwise vortex with an oblique shock wave by means of unsteady three-dimensional Euler equations. A mathematical model of the vortex is considered. Some elements of the technique developed and calculation results of interaction of the streamwise vortex with the oblique shock wave are presented.

1. Formulation of the Problem. A supersonic perfect-gas flow contains a streamwise vortex propagating from left to right. The velocities in the vortex core and in the cocurrent flow in the initial cross section are assumed to be supersonic. An oblique shock wave is located in a transverse plane inclined at a certain angle to the axis of the streamwise vortex (Fig. 1). To simplify problem formulation, we assume that the shock-wave generator is outside the computational domain. The axis of symmetry of the vortex is parallel to the free-stream velocity vector, and its direction coincides with the direction of the x axis. The supersonic velocity of the incoming flow is assumed to be constant and independent of time. The intensity of the streamwise vortex is characterized by vortex circulation Γ_0

and relative axial velocity Φ. The quantities Φ and Γ_0 are the governing parameters, their values are prescribed, i.e., the given parameters are the vortex circulation Γ_0 and the relative axial velocity $\Phi = V_x^0/V_\infty$ (V_x^0 is the flow velocity at the vortex axis and V_∞ is the flow velocity at infinity). We have to determine the flow structure in the case of interaction of the streamwise vortex and oblique shock wave. In determining parameters on the shock wave, it is assumed that the angle of the wedge generating the shock wave is prescribed, and thus, the angle of inclination of the shock wave is also given. The flow parameters at infinity are also specified.

The problem was solved within the framework of the inviscid ideal-gas flow with the use of three-dimensional unsteady Euler equations. Such an approach was chosen with allowance for the results of [6], where it was shown that the beginning of vortex-core breakdown on the shock wave seems to be independent of viscosity and is mainly determined by the relative streamwise component of velocity in the vortex core and by the angle of inclination of the shock wave. It is assumed that viscous effects have little influence on the geometric size of the interaction region; therefore, the main features of the flow structure, with allowance for the fact that viscosity is implicitly (because experimental results are used) present in the vortex model, is taken into account in the approach used. A more detailed flow structure can be obtained by using Navier–Stokes equations. A scheme of the Godunov method type is used to solve the system of equations considered. The method of Einfeldt [13] is applied to determine numerical fluxes at the boundaries of the computational cell. In the form described, the scheme has the second order of accuracy in terms of spatial variables. Some computations were performed with fourth-order accuracy in terms of spatial variables.

2. Vortex Model. For theoretical investigations of interaction of the streamwise vortex and the shock wave, its is necessary to construct a mathematical model of the vortex. It is desirable to have a vortex insulated from the external cocurrent flow (at least in the initial cross section). The simplest vortex models are constructed within the framework of an axisymmetric flow. In this formulation, the position of the vortex boundary can be arbitrary to a certain extent. In constructing the vortex-core model, a necessary aspect is the concentration of the major part of vorticity in the core. Such a model allows one to impose the boundary condition at the entrance of the computational domain in solving a three-dimensional problem of vortex interaction with an external disturbance (e.g., shock wave). The structure of a streamwise vortex formed behind a diamond-shaped body exposed to a supersonic flow was experimentally studied in [7, 9]. The results showed that the structure of the streamwise vortex being formed is close to the structure of the Burgers vortex. In the present work, the Burgers vortex model was supplemented by experimental dependences of the streamwise axial velocity in the vortex center on the vortex radius and flow velocity at infinity [4]. The distribution of quantities across the vortex is similar to the distribution of parameters in the classical Burgers vortex; a linear distribution of velocity is set in the vortex core and velocity decreases exponentially with distance from the vortex core. The tangential velocity V_θ in the Burgers vortex is written as

$$V_\theta = \Gamma_0(1 - \exp[-(r/r_c)^2])/r,$$

where Γ_0 is the vortex circulation and r_c is the vortex-core radius. Passing from the cylindrical coordinate system (x, r, θ) to the Cartesian coordinate system (x, y, z), we obtain expressions for the velocities v and w:

$$v = V_\theta \sin\theta, \qquad w = -V_\theta \cos\theta.$$

The distribution of the axial velocity in the vortex is determined from the generalization made on the basis of the experimental data of [4]:

$$V_x(r) = V_\infty + V_\infty(\Phi - 1)\exp[-(r/r_c)^2].$$

Here Φ is the ratio of velocity at the vortex axis to velocity at infinity. The pressure in the vortex cross section is calculated from the equation of conservation of momentum for the radial component

$$\frac{dp}{dr} = \frac{\rho V_\theta^2}{r},$$

where the radial component of velocity is assumed to be zero. In calculating density in the streamwise vortex, it was assumed that the total temperatures in the vortex and in the cocurrent flow are identical. This assumption is confirmed by the experimental data of [4], which show that the ratio of total temperatures in the vortex and in the cocurrent flow is within 0.95–1.05. With allowance for the assumptions made above, the differential equation for the pressure across the vortex is

$$\frac{dp}{dr} = \frac{\gamma}{\gamma - 1}\,\frac{p}{H_0 - 0.5(V_x^2 + V_\theta^2)}\,\frac{V_\theta^2}{r}$$

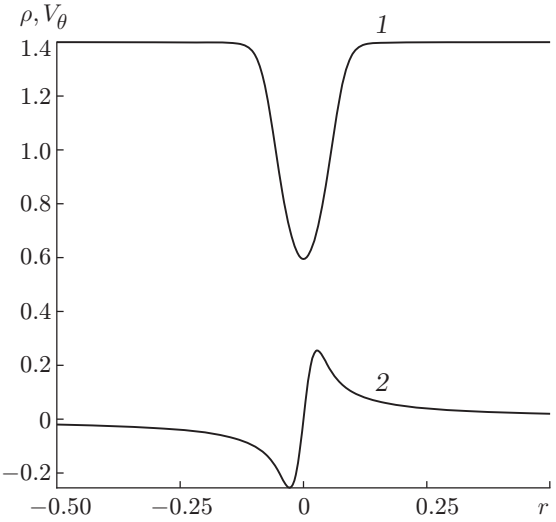

Fig. 2. Distributions of density (curve 1) and tangential component of velocity (curve 2) across the vortex.

(H_0 is the total enthalpy of the cocurrent flow). The resultant ordinary differential equation for pressure was solved by the sixth-order Runge–Kutta method.

Figure 2 shows the distributions of density and tangential velocity along the radius of the vortex modeled by the ordinary differential equation derived above. The calculations were performed with the following parameters: free-stream Mach number $\mathrm{M}_\infty = 3$, $\Gamma_0 = 0.4$, $\Phi = 0.6$, and ratio of specific heats $\gamma = 1.4$. In Fig. 2, the density is normalized to ρ_∞/γ, the velocity V_θ to the velocity of sound in the flow at infinity, and r to the size of the computational domain along the y axis (equal to 0.12 m). It follows from Fig. 2 that the azimuthal component of velocity increases with increasing radius, reaches a maximum at the vortex-core boundary, and then exponentially decreases. The flow density at the vortex center decreases almost by 2.7 times. The static pressure in the vortex core changes significantly weaker and is approximately 10% lower than the pressure in the ambient flow.

3. Governing Equations and Boundary Conditions. Let t be the time, ρ and p be the density and pressure, u, v, and w be the components of the velocity vector in the Cartesian coordinate system (x, y, z), $\boldsymbol{Q}$ be the vector of conservative variables, and $\boldsymbol{F}$, $\boldsymbol{G}$, and $\boldsymbol{H}$ be the vectors of convective fluxes. Three-dimensional equations that describe the flow of a compressible gas in the Cartesian coordinate system can be written as

$$\frac{\partial \boldsymbol{Q}}{\partial t} + \frac{\partial \boldsymbol{F}}{\partial x} + \frac{\partial \boldsymbol{G}}{\partial y} + \frac{\partial \boldsymbol{H}}{\partial z} = 0.$$

The vectors $\boldsymbol{Q}$, $\boldsymbol{F}$, $\boldsymbol{G}$, and $\boldsymbol{H}$ for a compressible gas flow have the following form:

$$\boldsymbol{Q} = (\rho, \rho u, \rho v, \rho w, E)^{\mathrm{t}}, \qquad \boldsymbol{F} = (\rho u, \rho uu + p, \rho vu, \rho wu, (E + p)u)^{\mathrm{t}},$$

$$\boldsymbol{G} = (\rho v, \rho uv, \rho vv + p, \rho wv, \rho h_0 v)^{\mathrm{t}}, \qquad \boldsymbol{H} = (\rho w, \rho uw, \rho vw, \rho ww + p, \rho h_0 w)^{\mathrm{t}}.$$

Here E is the total energy and h_0 is the total specific enthalpy. The system is supplemented by the equation of state in the form

$$p = (\gamma - 1)[E - \rho(u^2 + v^2 + w^2)/2].$$

To solve the system considered, we used the Godunov method. Numerical fluxes at the boundaries of the computational cell $\boldsymbol{F}_{i\pm1/2,j,k}, \boldsymbol{G}_{i,j\pm1/2,k}$, and $\boldsymbol{H}_{i,j,k\pm1/2}$ were obtained (i.e., the Riemann problem was solved) by the HLLEM method [13]. Let us consider the method for calculating numerical fluxes by an example of the vector $\boldsymbol{F}$. Numerical fluxes in other coordinate directions were calculated in a similar manner. In calculating numerical fluxes at the boundaries of the computational cell $\boldsymbol{F}_{i\pm1/2}$, we used the TVD methodology proposed in [14]. At this stage, the vector $\boldsymbol{q}^{r,l}_{i\pm1/2} = (\rho, u, v, w, p)^{\mathrm{t}}$ was calculated with the second order of approximation. Some calculations were

performed with fourth-order approximation of the vector $\boldsymbol{q}^{r,l}_{i\pm1/2}$ [14]. At the first stage, numerical fluxes at the cell boundaries were determined by the formulas

$$\boldsymbol{F}_{i+1/2} = \frac{b^+\boldsymbol{F}^l_i - b^-\boldsymbol{F}^r_{i+1}}{b^+ - b^-} + \frac{b^+b^-}{b^+ - b^-}\,(\boldsymbol{Q}^r - \boldsymbol{Q}^l),$$

$$b_l = \min\,(\hat{U} - \hat{c}, U_i - c_i), \qquad b_r = \max\,(\hat{U} + \hat{c}, U_{i+1} + c_{i+1}),$$

$$\delta = \hat{c}/(\hat{c} + |0.5(b_l + b_r)|), \quad b^+ = \max\,(b_r, 0), \quad b^- = \min\,(b_l, 0),$$

where U is the velocity component normal to the cell boundary; the values of $\hat{U}$ and $\hat{c}$ are calculated by the averaging technique of [15]. The subscripts l and r refer to the states on both sides of the interface separating the cells. For final determination of the numerical flux $\boldsymbol{F}_{i+1/2}$, we used the following modification of the method of [13]:

$$\boldsymbol{F}^{\rm mod}_{i+1/2} = \boldsymbol{F}_{i+1/2} - (b^+b^-/(b^+ - b^-))[\delta_{i+1/2}(\alpha^2_{i+1/2}\boldsymbol{R}^2_{i+1/2} + \alpha^3_{i+1/2}\boldsymbol{R}^3_{i+1/2} + \alpha^4_{i+1/2}\boldsymbol{R}^4_{i+1/2})].$$

Here $\boldsymbol{R}^k$ are the right-side eigen vectors of the matrix $\partial\boldsymbol{F}/\partial\boldsymbol{Q}$ and α^k are the coefficients of the expansion $\Delta\boldsymbol{Q} = \boldsymbol{Q}^r - \boldsymbol{Q}^l = \sum\alpha^k\boldsymbol{R}^k$ in terms of the right-side eigen vectors $\boldsymbol{R}^k$. The unsteady Euler equations were integrated with respect to time by the third-order explicit TVD Runge–Kutta scheme proposed in [16].

Constant parameters of a supersonic flow were set at the input boundary on the left. The left boundary was located far from the vortex–shock wave interaction region to avoid upstream influence of disturbances from the interaction region on the free-stream parameters. The conditions at the input boundary remained unchanged. Nonreflecting boundary conditions for hyperbolic systems of equations proposed in [17] were set at the output and upper boundaries of the computational domain. A modification of these boundary conditions for this particular three-dimensional problem was developed. In using the ideology of nonreflecting boundary conditions based on characteristic relations, it was assumed that the amplitudes of incoming waves are constant in time at the boundary, which is equivalent to the statement that there are no incoming waves. At the lower boundary with the incoming flow only, two additional rows of fictitious cells with constant gas-dynamic parameters equal to their initial values were set. It was assumed that the side boundaries are solid walls; therefore, the no-slip conditions were set there. In addition, these boundaries were moved away to a distance such that the reflected disturbance did not enter the vortex–shock wave interaction region.

The problem was solved in the region shaped as a parallelepiped. Test computations showed that it is necessary to use a grid adaptive to the flow structure in calculating vortex–shock wave interaction. Based on the solution of the ordinary differential equation for the vortex, the greatest gradients of parameters were observed in the vortex core. Therefore, an exponential distribution of grid nodes along the y and z axes with the origin in the vortex center was used in the entire computational domain. As a result of such a procedure, the grid in the vortex core was finer. In the x direction, the grid had a uniform step. All computations were performed on a $120 \times 90 \times 90$ grid along the x, y, and z axes, respectively.

4. Computation Results. Numerical simulation of the flow structure in the case of interaction of a streamwise vortex with an oblique shock wave was performed in the range of free-stream Mach numbers $\mathrm{M}_\infty = 3$–5. It was assumed that the streamwise direction of the vortex axis coincides with the direction of the x axis. It was also assumed that the direction of the flow velocity vector ahead of the shock-wave front coincides with the direction of the x axis. The variable parameters were the vortex circulation Γ_0 and the axial streamwise velocity of the vortex. Flow regimes with variation of the angle of the wedge generating the shock wave were also considered. The wedge angle was varied within the range $\theta = 23$–$30°$, which led to an increase in shock-wave strength. The computations were performed for the following geometric dimensions of the domain: length of 0.24 m, height and width of 0.12 m, and vortex radius $r_c = 0.03$ m. It was assumed in the computations that the absolute values of the free-stream parameters (pressure and density) were unchanged in time: $p = 1171.84$ N/m^2 and $\rho = 0.014\,76$ kg/m^3. The geometric parameters of the incoming streamwise vortex were also assumed to be unchanged. The experimental and numerical investigations of vortex–shock wave interaction show that a drastic increase in the cross-sectional size of the vortex (vortex breakdown) in the region of its interaction with the shock wave depends mainly on velocity deficit. Therefore, one of the basic parameters of the problem is the relative streamwise velocity Φ. Depending on Φ, the interaction structure was essentially different. The computation results revealed three modes of interaction of the streamwise vortex with the shock wave (weak, moderate, and strong) depending on the combination of the governing parameters M_∞, Γ_0, Φ, and θ.

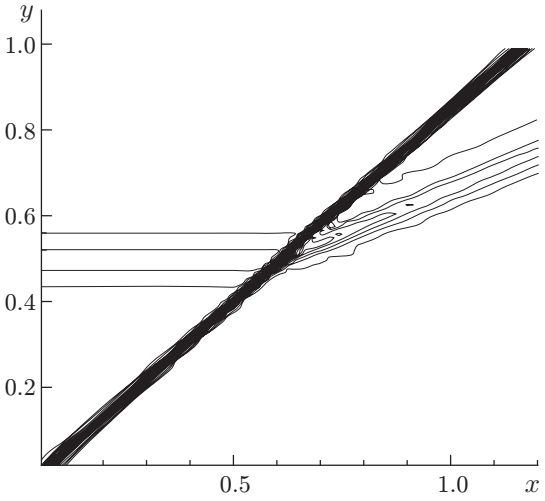

Fig. 3. Isolines of density in the yx plane in the case of weak interaction ($M_\infty = 3$).

Weak Interaction. Figure 3 shows a typical example of the weak mode of interaction of the streamwise vortex and oblique shock wave. The flow structure is shown in the yx plane passing through the axis of the incoming vortex. The computation was performed for the following flow parameters: $M_\infty = 3$, $\Gamma_0 = 0.4$, $\Phi = 1.0$, and $\gamma = 1.4$. The shock wave in Fig. 3 has the form of condensed isolines of density, which are almost straight lines inclined to the horizontal axis at a constant angle. The angle of the wedge generating the shock wave is 23.3°. The vortex incoming onto the shock wave is presented in the form of sectors of horizontal straight lines near the axis of symmetry. It follows from Fig. 3 that the vortex passes through the shock wave and, interacting with the latter, turns at a certain angle; the axis of symmetry of the vortex becomes parallel to the velocity vector behind the shock wave (actually, the vortex propagates along the wedge generating the shock wave). It follows from the computation results that the vortex remains almost undistorted when passing through the shock wave. The vortex shape in the yz cross section behind the shock-wave front changes weakly and is close to a circle. The shock-wave shape does not change significantly either. The slope of the shock wave also remains almost unchanged. As a result of weak interaction, the flow in the entire computational domain remains supersonic. Thus, weak interaction is characterized by weak distortion of the shock-wave front, minimum change in the vortex structure, and supersonic velocity in the entire flow region. The flow structure is unchanged in time. This agrees with the experimental data of [4], which also show that the flow structure in the case of weak interaction remains unchanged in time.

Moderate Interaction. Another type of streamwise vortex–shock wave interaction is observed with decreasing streamwise velocity at the axis of symmetry of the incoming vortex, i.e., with decreasing parameter Φ. In terms of the action on the shock wave, this type can be called moderate. As an example of the moderate interaction mode, we give the computation results for the following initial parameters: $M_\infty = 3$, $\Gamma_0 = 0.4$, $\Phi = 0.8$, and $\gamma = 1.4$. Figures 4 and 5 show the computation results for the moderate type of vortex–shock wave interaction. In this case, the shock-wave front becomes significantly curved (see Fig. 4). The greatest deviation from the shape of the bow shock wave is observed at the point of intersection of the vortex centerline with the shock wave, where the shock-wave front, being curved, becomes perpendicular to the vortex centerline. This indicates that a normal shock is formed in this region, and a subsonic flow region should appear behind this wave.

The computations show that a local three-dimensional subsonic flow region appears behind the leading front of the shock wave and propagates downstream at a certain positive angle to the axis of the incoming vortex. There are no reverse flows in the closed subsonic flow region, and the streamwise component of velocity is always positive there. The mean angle of deviation of the subsonic region axis is 3–4° greater than the wedge angle. The presence of the subsonic region is caused by the fact that the Mach number is minimum at the vortex centerline. The static pressure in the vortex core is close to the free-stream pressure. When the flow with a locally low Mach number hits the shock wave, the pressure difference on the latter should be significantly smaller than that on an undisturbed shock wave. To obtain the same level of pressure behind the vortex–shock wave interaction region as that in the free

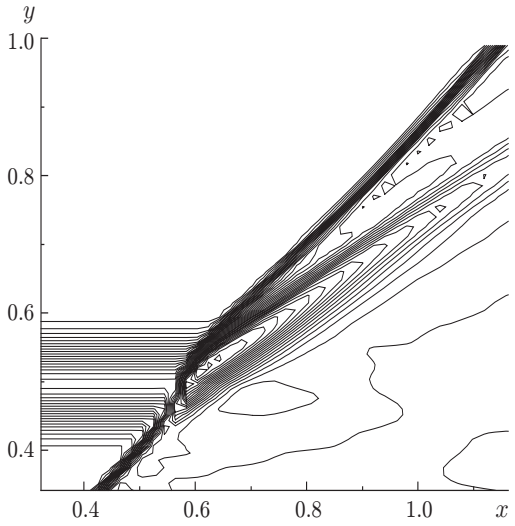

Fig. 4

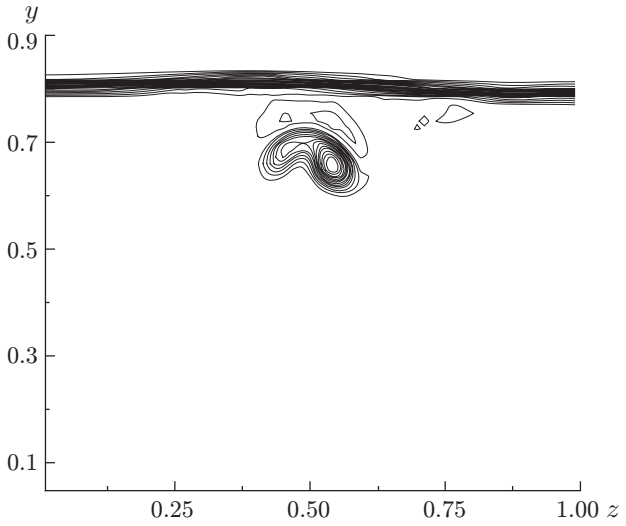

Fig. 5

Fig. 4. Mach number isolines in the yx plane in the case of moderate interaction ($M_\infty = 3$).

Fig. 5. Mach number isolines in the yz plane in the case of moderate interaction ($M_\infty = 3$).

stream, flow reconstruction in the interference region is necessary. The transition from low pressure to significantly higher pressure can be performed either in a system of shock waves or in the normal shock. Thus, vortex–shock wave interaction results in structural reconstruction of the flow in the vicinity of the vortex core. In particular, in the moderate interaction mode, this leads to the formation of the normal shock in the vortex core.

The numerical results for the moderate interaction regimes show that the increase in static pressure along the vortex axis in the undisturbed flow, as compared to the pressure in the subsonic region, corresponds to the pressure difference on the normal shock. The following features of the flow structure can be noted in the yz plane (for $x = 0.94$). The chosen cross section is located behind the front of the main shock wave. In contrast to the weak interaction mode, the following features are observed in the yz plane (see Fig. 5): passing through the shock-wave front, the primary streamwise vortex separates into two weakly connected vortices. The vortices rotate in the opposite directions. The right and left vortices rotate in the clockwise and counterclockwise directions, respectively. The vortices are located at identical distances from the plane of symmetry and have an almost ellipsoidal shape. In the case of moderate interaction, the core is supersonic in one vortex and subsonic in the other. As the x coordinate increases (i.e., with distance from the shock wave), the area occupied by the subsonic flow in the vortex in the yz cross section decreases. The observed effect of vortex separation is confirmed by the experimental data of [8].

Strong Interaction. Figures 6 and 7 show the computation results for strong interaction of the streamwise vortex with the oblique shock wave. In this case, drastic changes in the shock-wave shape and parameters of the incoming streamwise vortex ahead of the shock wave are observed. Because of the low values of the total pressure, Mach number in the vortex core, and angle of inclination of the velocity vector to the shock wave, the shock-wave front and the flow structure in the interaction region ahead of the front become substantially different. In the case of strong interaction, the shape of the shock-wave front in the interference region differs from the straight line. A local zone of subsonic recirculation flow is formed, which is located upstream of the initial position of the shock-wave front at a certain distance depending on the governing parameters.

Figure 6 shows the flow structure in the case of strong interaction of the streamwise vortex with the shock wave in the yx plane for $M_\infty = 3$, $\Gamma_0 = 0.4$, $\Phi = 0.6$, and $\theta = 29°$. Recirculation flow regions are visible ahead of the main shock wave in the yx plane. It follows from the computation results that the flow in these regions is subsonic. The static pressure in the recirculation region is 2–3 times higher than the free-stream pressure. A shock wave is formed around the recirculation region. This region can be considered as a certain blunted solid body exposed to a supersonic nonuniform flow. In the case of a supersonic flow around a blunted body, a detached shock wave with a subsonic flow region behind is formed ahead of the body (at a certain distance). In the case of interaction of the streamwise vortex and the shock wave, there is an asymmetric closed subsonic recirculation flow region near the

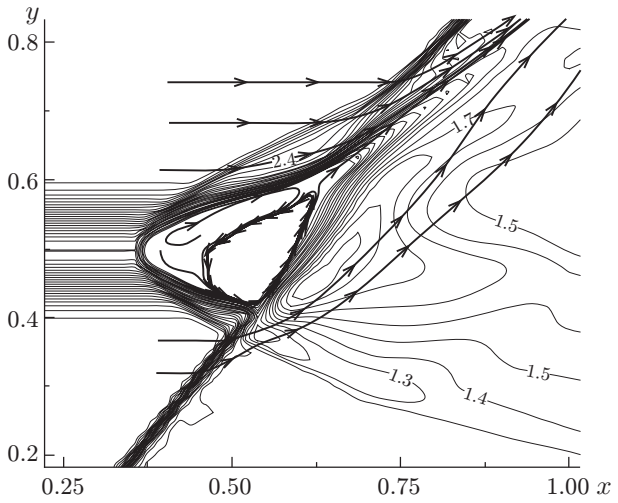

Fig. 6

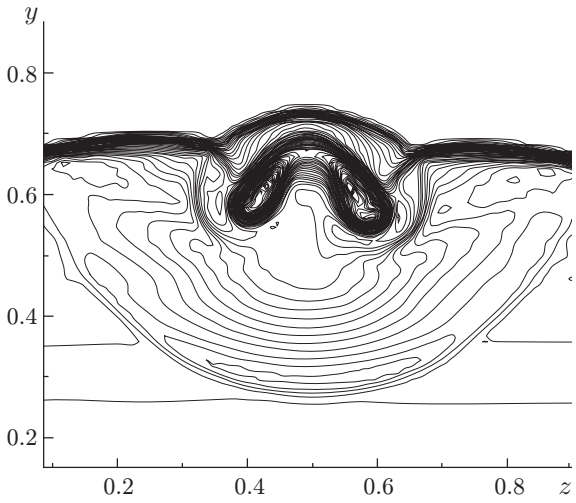

Fig. 7

Fig. 6. Mach number isolines and streamlines in the yx plane in the case of strong interaction ($M_\infty = 3$).

Fig. 7. Mach number isolines in the yz plane in the case of strong interaction ($M_\infty = 3$).

axis of symmetry. Between the normal shock and recirculation region, there is a point with zero flow velocity at the vortex axis. The angle of inclination of the shock wave formed around the recirculation-flow region to the vortex axis is variable, since the Mach number in the vortex core increases significantly in the direction away from its axis (at the axis of symmetry, the shock-wave front is perpendicular to the vortex axis). With distance from the axis of symmetry, the slope of the shock-wave front decreases. At the exit from the vortex, the shock-wave shape is close to conical. After that, the conical shock wave interacts with the main shock wave formed by the wedge.

Thus, in the case of strong interaction, there arises a three-dimensional subsonic reverse flow region ahead of the front of the main shock wave. In its structure, this region is similar to the separated flow region arising, for instance, in the viscous supersonic flow around a compression corner. The emergence of the reverse flow region leads to significant expansion of the vortex cross section. In all examined regimes of strong interaction, a subsonic reverse flow region was observed, which was separated from the supersonic flow region by a slip surface over the entire perimeter.

The flow is supersonic in the region between the slip surface and the shock wave formed ahead of the recirculation region and subsonic under the slip surface. The contact streamline (if we consider the flow structure in the yx plane) emanates from the point on the formed conical shock wave in which the Mach number is $M = 1$ behind the front. The presence of the slip surface is confirmed by computation results, which show that the density and Mach number above and below the slip surface are significantly different, whereas the values of pressure are almost coincident. The size of the reverse flow region depends on the shock-wave strength, i.e., on the angle of the wedge generating the shock wave. The length of the local subsonic flow region can serve, to a certain extent, as a characteristic of the strong interaction mode. As in the case of weak interaction, rarefaction regions appear behind the shock wave in the case of strong interaction. This leads to a decrease in pressure on the wedge surface as compared to the pressure arising in a uniform supersonic flow around the wedge; this decrease is more significant in the case of strong interaction. Thus, the pressure on the wedge in the case of strong interaction is lower than that in the case of weak interaction.

The following features of the flow structure behind the recirculation flow region ($x = 0.74$) in the yz plane can be noted. In the yz cross section, one can see the conical shock wave arising ahead of the recirculation region with the center at $z = 0.5$ and the adjacent main shock wave (see Fig. 7). Splitting of the primary streamwise vortex into two vortices is also observed (see Fig. 7). The presence of two vortices is confirmed by a significant decrease in density in them and by the change in the direction of the velocity vector over the vortex perimeter. The vortices rotate in the opposite directions: the right vortex rotates clockwise and the left vortex rotates counterclockwise. The vortices are located at identical distances from the plane of symmetry and have an almost ellipsoidal shape. In

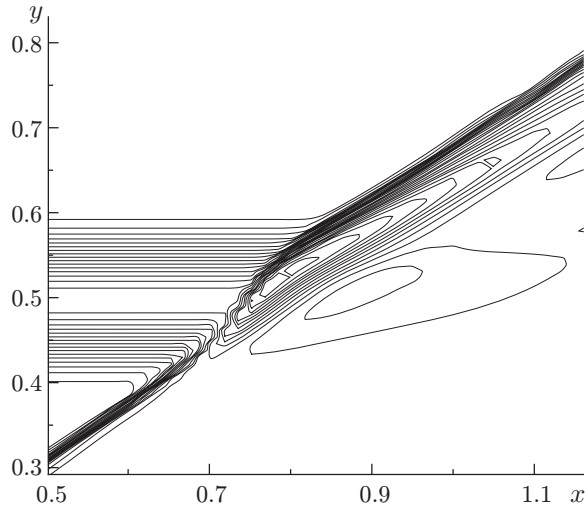

Fig. 8

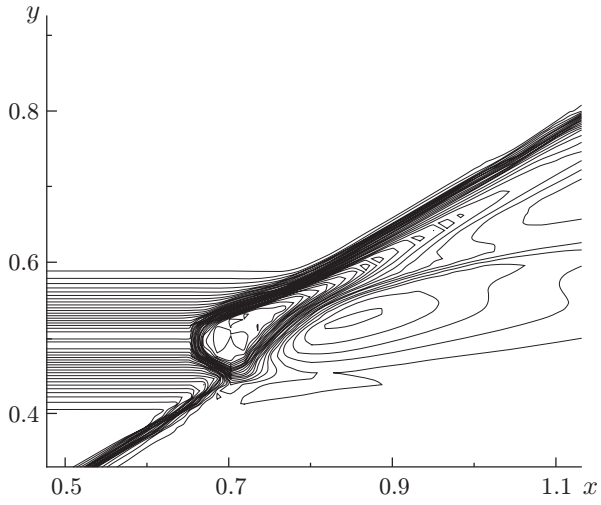

Fig. 9

Fig. 8. Mach number isolines in the yx plane in the case of weak interaction ($M_\infty = 5$ and $\Gamma_0 = 0.4$).
Fig. 9. Mach number isolines in the yx plane in the case of strong interaction ($M_\infty = 5$ and $\Gamma_0 = 2$).

contrast to the moderate interaction mode, the cores of both vortices are subsonic in the case of strong interaction. Comparing the positions of the right or left split vortex in the yz plane at different x distances, one should note the following: 1) the axis of the split vortices is inclined to the x axis at a positive angle; 2) with increasing x coordinate, the major axis of the ellipse of the left vortex starts to turn counterclockwise, whereas the major axis of the right vortex turns clockwise. With increasing x coordinate (i.e., with distance from the shock-wave front), the area occupied by the subsonic flow in the vortex in the yz cross section decreases.

In the present work, we studied the effect of circulation Γ_0 of the streamwise vortex on the type of its interaction with the shock wave. The computations were performed for $M_\infty = 5$, $\Phi = 0.8$, and $\theta = 23.3°$. The computation results show that vortex circulation affects the type of interaction. Thus, the weak type of interaction is observed for $\Gamma_0 = 0.4$ (Fig. 8), and the strong type of interaction is observed for $\Gamma_0 = 2$ (Fig. 9). It should be noted, however, that vortex "explosion" (i.e., significant increase in its cross-sectional size) does not occur (Fig. 9). It follows from Fig. 9 that the recirculation region is located in the vortex core. This agrees with the experimental results of [8], where the same result was obtained for interaction of the streamwise vortex and the normal shock. The computation results show that the effect of the parameter Γ_0 on the interaction type is significantly weaker than the effect of the parameter Φ.

The angle of the wedge θ forming the shock wave exerts a more significant effect on the flow structure. The influence of this parameter on the flow structure in the case of interaction of the streamwise vortex with the shock wave is similar to the action of the parameter Φ. The influence of the parameter θ was considered for $M_\infty = 3$, $\Phi = 0.8$, and $\Gamma_0 = 0.4$. The computation results show that the flow structure for $\theta = 23.3°$ can be characterized as the weak interaction type. Already for $\theta = 25°$, however, the strong interaction type is observed, and for $\theta = 27°$, the flow contains recirculation regions of significant length. A further increase in θ leads to the emergence of a subsonic flow at the left boundary of the computational domain. The computation results obtained agree with the experimental data of [9].

5. Conclusions. Results of numerical investigations of the interaction of a streamwise vortex with an oblique shock wave are presented. A mathematical model of the streamwise vortex is constructed. Three types of interaction (weak, moderate, and strong) are revealed. It is shown that vortex breakdown is possible in the case of strong interaction. The effect of vortex breakdown is characterized by a significant change in its structure: a subsonic recirculation region appears and the vortex diameter substantially increases. It is demonstrated that the major influence on the interaction type is exerted by the streamwise velocity and the angle of the wedge generating the shock wave. The effect of splitting of the primary vortex on the shock wave in moderate and strong interaction regimes is found.

This work was supported by the Russian Foundation for Fundamental Research (Grant No. 02-01-01265).

REFERENCES

1. M. D. Brodetsky, E. Krause, S. B. Nikiforov, et al., "Evolution of vortex structures on the leeward side of a delta wing," *J. Appl. Mech. Tech. Phys.*, **42**, No. 2, 243–254 (2001).
2. B. A. Lugovtsov, "Asymptotic behavior of the far region of turbulent wake vortices," *J. Appl. Mech. Tech. Phys.*, **40**, No. 2, 198–207 (1999).
3. S. Leibovich, "Vortex stability and breakdown: survey and extention," *AIAA J.*, **22**, No. 9, 1192–1206 (1983).
4. J. M. Delery, "Aspects of vortex breakdown," in: *Progress in Aerospace Sciences*, Vol. 30, Pergamon Press, Oxford (1994), pp. 1–59.
5. V. V. Zatoloka, A. K. Ivanyushkin, A. V. Nikolaev, "Interference of vortices with shock waves in the inlet. Vortex breakdown," *Uch. Zap. TsAGI*, **6**, No. 2, 134–138 (1975).
6. G. F. Glotov, "Interference of a vortex core with shock waves in free flow and nonisobaric jets," *Uch. Zap. TsAGI*, **20**, No. 5, 21–32 (1989).
7. I. Kalkhoran, "Vortex distortion during vortex-surface interaction in a Mach 3 stream," *AIAA J.*, **32**, No. 1, 123–129 (1994).
8. L. N. Cattafesta and G. Settles, "Experiments on shock vortex interaction," AIAA Paper No. 92-0315 (1992).
9. M. K. Smart and I. Kalkhoran, "Effect of shock strength on oblique shock-wave vortex interaction," *AIAA J.*, **33**, No. 11, 2137–2143 (1995).
10. A. Nedungadi and M. J. Lewis, "Computational study of the flowfields associated with oblique shock vortex interactions," *AIAA J.*, **34**, No. 12, 2545–2553 (1996).
11. D. P. Rizzetta, "Numerical investigation of supersonic wing-tip vortices," *AIAA J.*, **34**, No. 6, 1203–1208 (1996).
12. G. Corpening and J. D. Anderson, "Numerical solutions to three-dimensional shock wave/vortex interaction at hypersonic speeds," AIAA Paper No. 89-0674 (1989).
13. B. Einfeldt, "On Godunov-type methods for gas dynamics," *SIAM J. Numer. Anal.*, **25**, No. 2, 294–318 (1988).
14. S. Yamamoto and H. Daiguji, "Higher-order-accurate upwind schemes for solving the compressible Euler and Navier–Stokes equations," *Comput. Fluids*, **22**, 259–270 (1993).
15. P. L. Roe, "Approximate Riemann solvers, parameter vectors, and difference schemes," *J. Comput. Phys.*, **43**, No. 2, 357–372 (1981).
16. C. W. Shu and S. Osher, "Efficient implementation of essentially non-oscillatory shock-capturing schemes," *J. Comput. Phys.*, **77**, No. 2, 439–471 (1988).
17. K. W. Thompson, "Time-dependent boundary conditions for hyperbolic systems," *J. Comput. Phys.*, **68**, No. 1, 1–24 (1987).